Electronic Supplementary Information (ESI)

Terephthalic Acid Induced Binder-free NiCoP-carbon Nanocomposite for Highly Efficient Electrocatalysis of Hydrogen Evolution Reaction

Suchada Sirisomboonchai[a,b], Shasha Li[a,b,c], Akihiro Yoshida[a], Suwadee Kongparakul [d], Chanatip Samart[d], Yasuki Kansha[e], Xiaogang Hao[c], Abuliti Abudula[b], Guoqing Guan[a,*]

[a]Energy Conversion Engineering Laboratory, Institute of Regional Innovation (IRI), Hirosaki University, 2-1-3, Matsubara, Aomori 030-0813, Japan.

[b]Graduate School of Science and Technology, Hirosaki University, 1-Bunkyocho, Hirosaki 036-8560, Japan.

[c]Department of Chemical Engineering, Taiyuan University of Technology, Taiyuan 030024, China.

[d]Department of Chemistry, Faculty of Science and Technology, Thammasat University, Pathumtani 12120 Thailand

[e]Graduate School of Arts and Sciences, College of Arts and Sciences, The University of Tokyo, 3-8-1 Komaba, Meguro, Tokyo 153-8902, Japan

* E-mail: guan@hirosaki-u.ac.jp

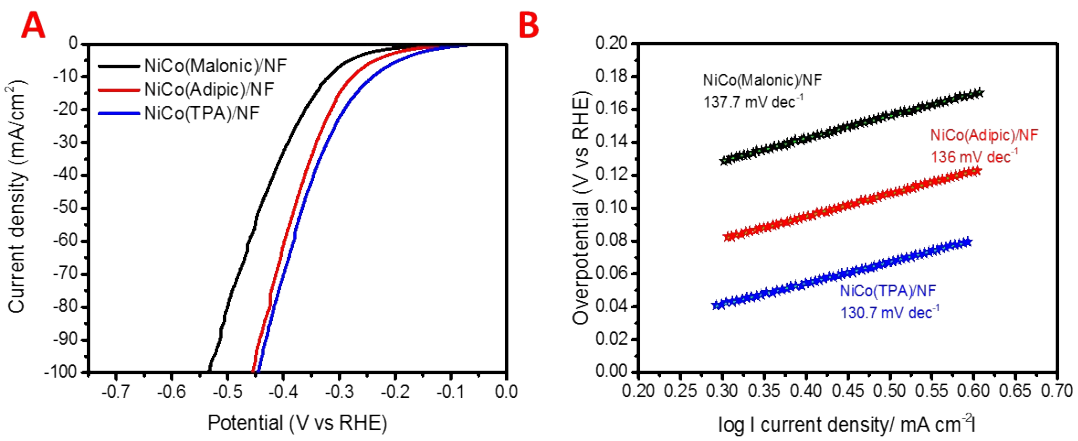

Figure S1. Electrochemical evaluation of three organic acid derived NiCo(organic compound) films on nickel foam electrode before calcination: (A) LSV polarization curves for HER; (B) Tafel slopes in 1.0 M KOH electrolyte at a scan rate of 1 mV s^{-1}.

Table S1. Summary of the overpotentials @ 10 mA cm^{-2} current density and the corresponding Tafel slope of the three organic acid derived NiCo(organic compound) films on nickel foam electrodes in **Figure S1**.

Electrode	Organic acid	Overpotential (mV @10mA/cm^2)	Tafel slope ($mVdec^{-1}$)
NiCo(Malonic)/NF	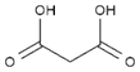	320	137.7
NiCo(Adipic)/NF	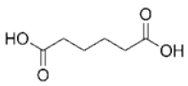	277.4	136
NiCo(TPA)/NF	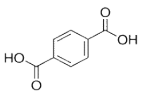	232	130.7

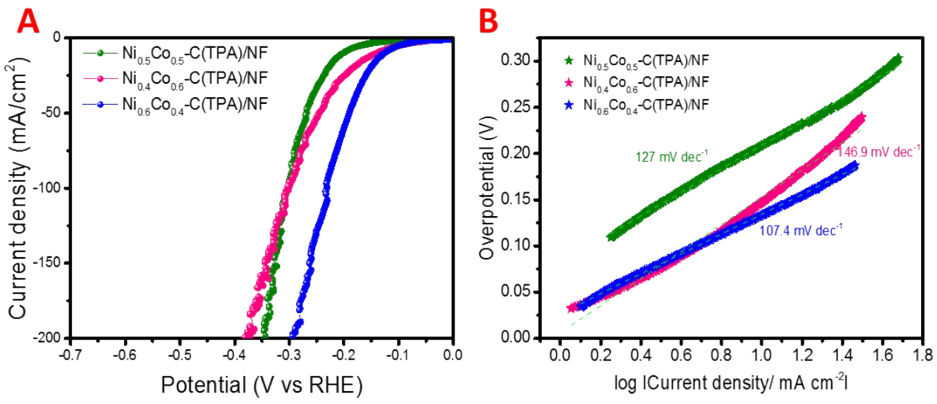

Figure S2. Electrochemical evaluation of NiCo-C(TPA)/NF electrodes with different mole ratios of Ni/Co: (A) LSV polarization curves for HER; (B) Tafel slopes in 1.0 M KOH electrolyte at a scan rate of 1 mV s^{-1}.

Table S2. Summary of the overpotentials @ 10 mA cm^{-2} current density and the corresponding Tafel slopes of NiCo-C(TPA)/NF electrodes with different Ni/Co molar ratios in Figure S2

Electrode	**Overpotential (mV@10mA/cm^2)**	**Tafel slope (mVdec^{-1})**
$Ni_{0.5}Co_{0.5}$-C(TPA)/NF	208	127
$Ni_{0.4}Co_{0.6}$-C(TPA)/NF	147	146.9
$Ni_{0.6}Co_{0.4}$-C(TPA)/NF	133	107.4

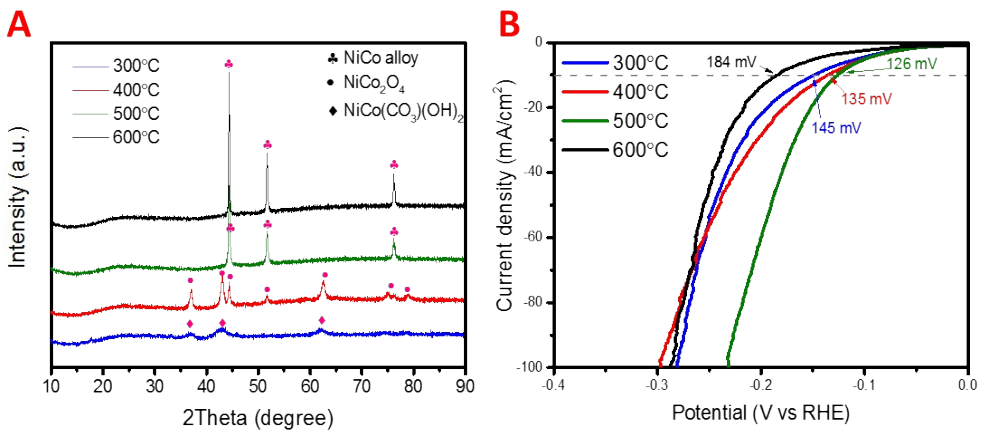

Figure S3. (A) XRD patterns of NiCo-C(TPA) carbonized at different temperatures and (B) LSV polarization curves of the obtained NiCo-C(TPA)/NF electrodes with different carbonization temperatures.

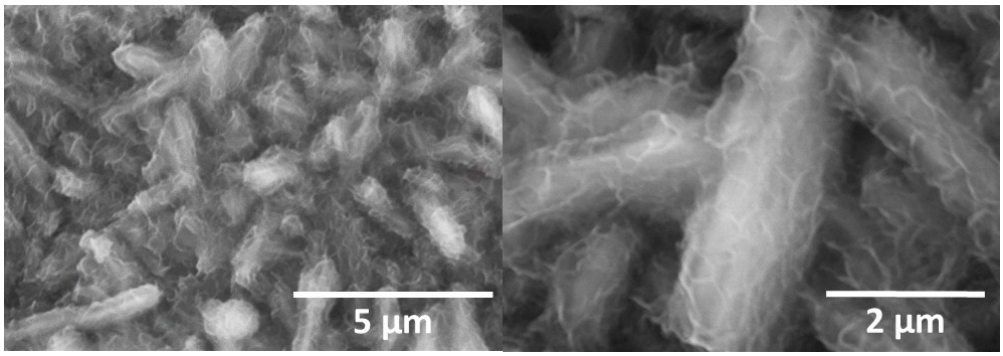

Figure S4. SEM image of NiCo-(TPA) film after the hydrothermal synthesis but without calcination process.

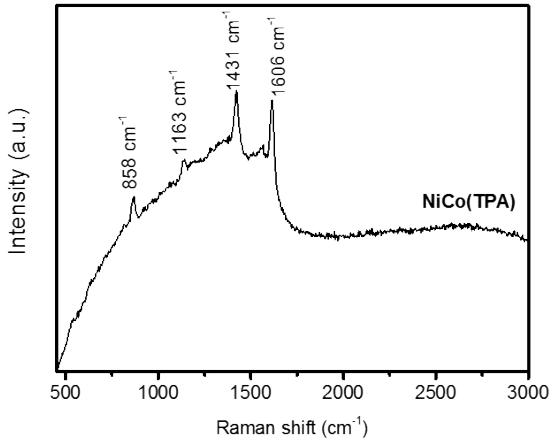

Figure S5. Raman spectra of NiCo(TPA) before calcination.

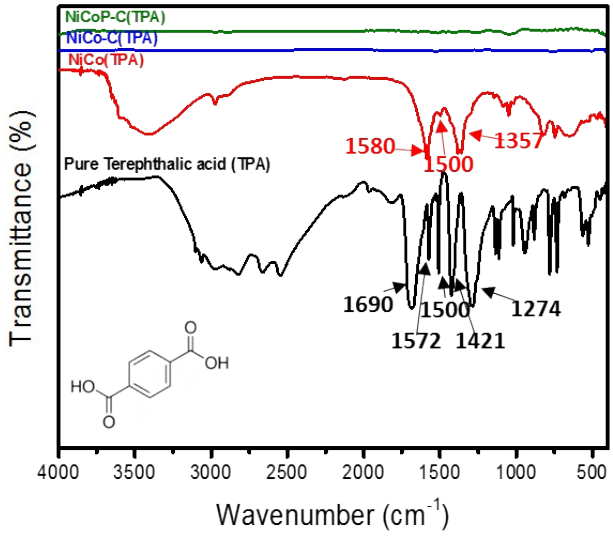

Figure S6. FT-IR spectra of pure terephthalic acid (TPA), NiCo(TPA) before calcination, NiCo-C(TPA) and NiCoP-C(TPA)

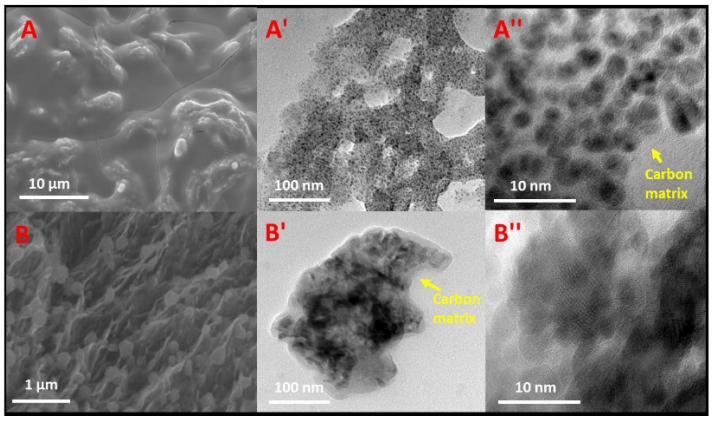

Figure S7. SEM images of (A) NiP-C(TPA) (B) CoP-C(TPA). TEM images of (A', A") NiP-C(TPA) and (B', B") CoP-C(TPA).

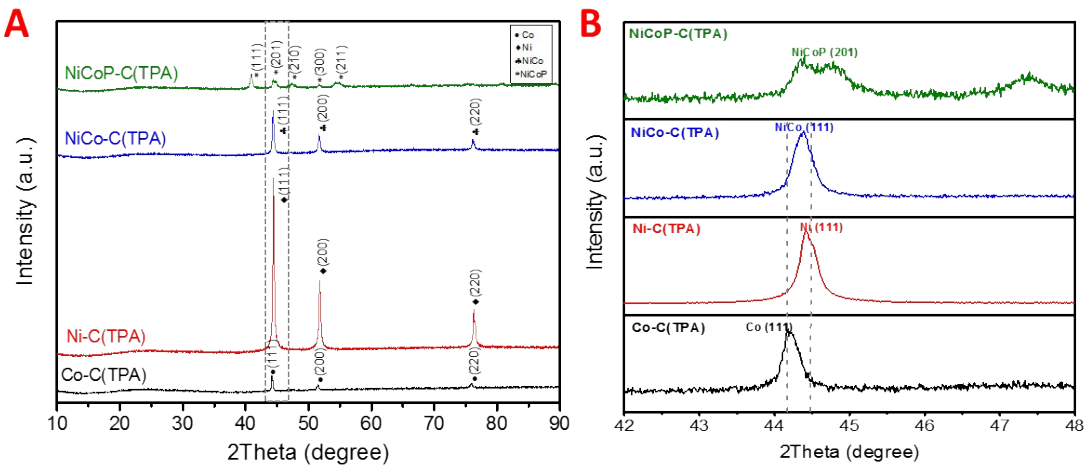

Figure S8. (A) XRD patterns of Co-C(TPA), Ni-C(TPA), NiCo-C(TPA) and NiCoP-C(TPA). (B) The corresponding magnification region with 2Θ ranging from 42º to 48º.

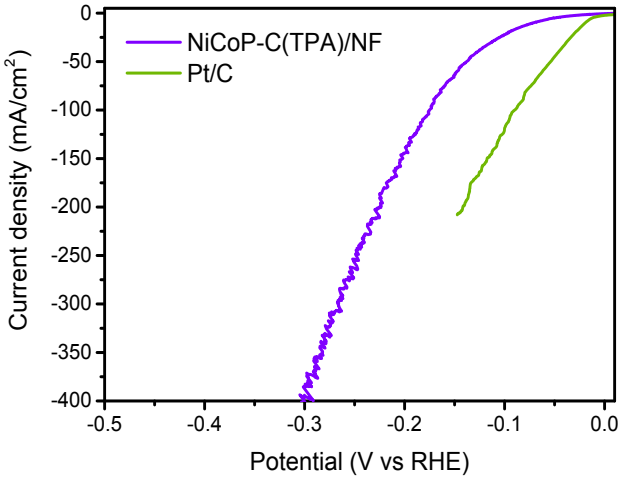

Figure S9. Electrocatalytic HER performance of NiCoP-C(TPA)/NF compared with that of 20 wt% Pt/C electrode at a scan rate of 1 mV s-1 in 1M KOH electrolyte.

Table S3. Comparison of this work with other related electrocatalysts working in alkaline electrolyte in the literatures

Electrocatalyst	Overpotential (mV) @10mA/cm^2	Tafel slope (mVdec^{-1})	Electrolyte	Electrode	Ref.
NiCoP-C(TPA)/NF	78	73.4	1 M KOH	Nickel foam	This work
NiCo-MOF	180	168	0.1 M KOH	Nickel foam	1
NiCoFe-MOF	110	114	0.1 M KOH	Nickel foam	1
Ni_2P-CoP	105	64	1 M KOH	Glassy carbon	2
Ni_2P	137	67	1 M KOH	Glassy carbon	2
CoP	184	66	1 M KOH	Glassy carbon	2
C@Ni_8P_3	114	59	1 M KOH	Nickel foam	3
Ni-Co-P	150	60.6	1 M KOH	Nickel foam	4
NiCoP/CC(Nest-like)	62	68.2	1 M KOH	Carbon cloth	5
CoP/CC	290	115.9	1 M KOH	Carbon cloth	5
NiP_2 NS/CC	102	64	1 M KOH	Carbon cloth	6
CoP/rGO	150	38	1 M KOH	Glassy carbon	7
Ni_2P/Ni/NF	98	72	1 M KOH	Nickel foam	8
$Cu_{0.3}Co_{0.2}P$	220	122	1 M KOH	Glassy carbon	9
Mn-CoP	95	53	1 M KOH	Carbon rod	10
Pt/C	32	33	1 M KOH	Pt foil	11

.

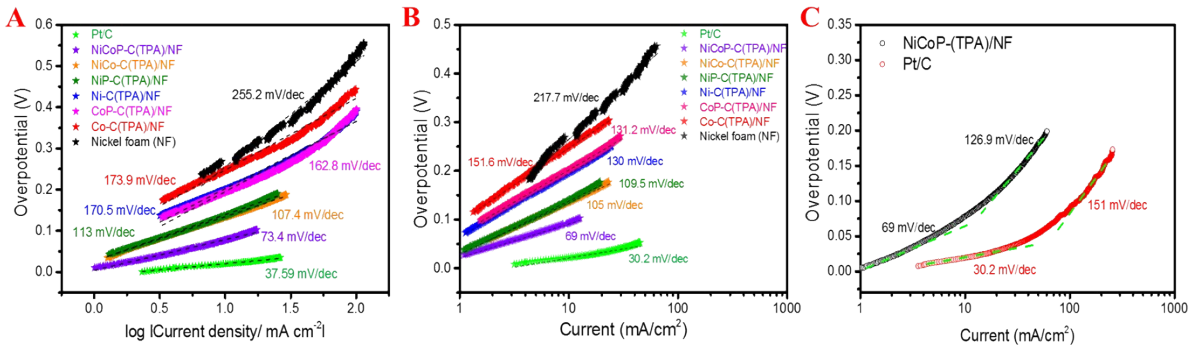

Figure S10 (A) Tafel curves converted from voltammogram. (B) Tafel curves obtained by direct measuring the Tafel characteristics using the electrochemical workstation. (C) Estimated Tafel data for evaluation of the reaction rate determining step (selection of NiCoP-(TPA)/NF and 20%wt Pt/C coated NF as the examples).

Table S4. Comparison Tafel slopes from two different techniques based Figure S10.

Catalyst	Tafel slope from voltammogram	Tafel slope directly from electrochemical station
20%wt Pt/C	37.59	30.2
NiCoP-C(TPA)/NF	73.4	69
NiCo-C(TPA)/NF	107.4	105
NiP-C(TPA)/NF	113	109.5
CoP-C(TPA)/NF	162.8	130
Ni-C(TPA)/NF	170.5	131.2
Co-C(TPA)/NF	173.9	151.6
Nickel foam (NF)	255.2	217.7

Conventionally, the Tafel analysis include two important parameters: the Tafel slope and the exchange current density. Empirically, the following Tafel relation has been well confirmed:

$$\eta = a + b \log(j)$$

The mechanism of HER includes the Volmer-Heyrovsky or Volmer-Tafel mechanism. In high pH alkaline media solution, the following reactions are suggested:.

$$H_2O + e^- + A \rightarrow AH_{ads} + OH^- \text{ (Volmer step)}$$

$$AH_{ads} + H_2O + e^- \rightarrow H_2 + OH^- + A \text{ (Heyrovsky reaction)}$$

$$AH_{ads} + AH_{ads} \rightarrow H_2 + 2A \text{ (Tafel reaction)}$$

where, A represents the hydrogen adsorption site and AH_{ads} represents the adsorbed hydrogen atom at the site. Theoretically, the Tafel slopes of 30-40 and near 120 mV dec^{-1} correspond to Heyrovsky and Volmer determining rate steps, respectively.[12] Especially, a Tafel slope of 120 mV dec^{-1} will be observed when the surface species is formed in the step just before the rate-determining one is predominant, and in other cases, the Tafel slope should be lower than 120 mV dec^{-1}. [13]

The Tafel slope from polarization voltammogram is the most common way to achieve the Tafel slope value, in which the polarization curve can be replotted as overpotential vs log (current density) and the Tafel slope can be determined via the linear relation. In this case, to avoid the experimental inaccuracy in Tafel slope, the low scan rate 1 mV/s is usually selected. Meanwhile, since a large amount of H_2 bubbles will be generated at the high overpotential, the Tafel slope is always determinded from the potential range at low overpotential to avoid the possible inaccuracy.[14]

Tafel slope can be also directly measured by an electrochemical workstation (Potentiostat) with a three electrode system in 1 M KOH electrolyte, in which carbon rod, Hg/HgO electrode and the prepared electrode are used as the counter electrode, reference electrode and working electrode, respectively. In this case, to detemine the Tafel slop, we estimated it by remaining the potential range as that in the LSV test with a step height of 0.5 mV, a step time of 3 s and a ultra-low scan rate of 0.1 mV/s. Herein, the Tafel slope can give information on the rate determining step directly.

As shown in Figure S10, the Tafel slopes of NiCoP-C(TPA)/NF and Pt/C mesured from the Tafel curves derived from LSV collected at a low scan rate of 1 mV/s at ambient conditions were 73.4 mV/dec and 37.59 mV/dec, respectively. In comparison, the Tafel slope directly mesured from the potentiostat workstation were 69 mV/dec and 30.2 mV/dec (which is close to the theoretical Tafel slope Pt/C, i.e., 30 mV/dec), respectively. It can be concluded that the difference of the Tafel slopes by using the two methods was not so significance (Table S4).

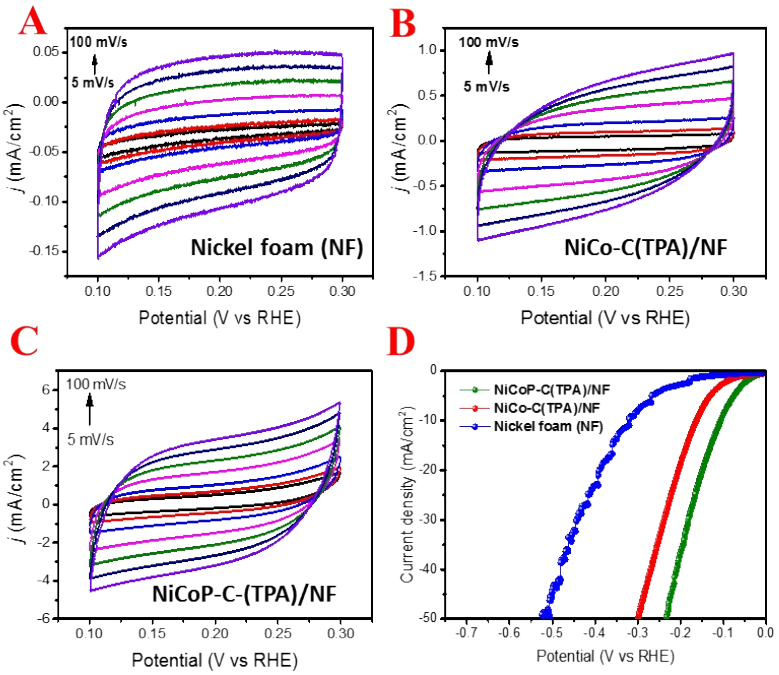

Figure S11. Cyclic voltammograms of (A) nickel foam (NF), (B) NiCo-C(TPA)/NF, (C) NiCoP-C(TPA)/NF collected between a potential range of 0.1-0.3V (vs RHE) with scan rates of 5, 10, 20, 40, 60, 80, 100 mV/s, respectively in 1 M KOH electrolyte. (D) LSV polarization curve normalized based on ECSA.

Table S5. Calculated ECSA and roughness of surface (R_f) of the samples in Figure S10.

Electrode	Cdl (mF cm^{-2})	Cs (mF cm^{-2})	ECSA ($\times 10^3$)	GSA (cm^2)	Rf ($\times 10^3$)
Nickel foam (NF)	1.9	0.04	0.0475	1.00	0.0475
NiCo-C(TPA)/NF	12.8	0.04	0.320	1.00	0.320
NiCoP-C(TPA)/NF	60	0.04	1.500	1.00	1.500

Calculation of electrochemical active surface area

The calculation of ECSA and roughness factor (R_f) by the follow equations:

$$ECSA = C_{dl}/C_s$$

$$R_f = ECSA/GSA$$

C_{dl} is the measured double layer capacitance of sample in 1.0 M KOH electrolyte (mF/cm^2)

C_s is the specific capacitance of a typical "value" for these materials, and all use the general specific capacitance (i.e., C_s = 0.04 mF cm^{-2} in 1.0 M KOH electrolyte).

ECSA is electrochemically active surface area.

R_f is roughness factor

GSA is geometric surface area of the sample.

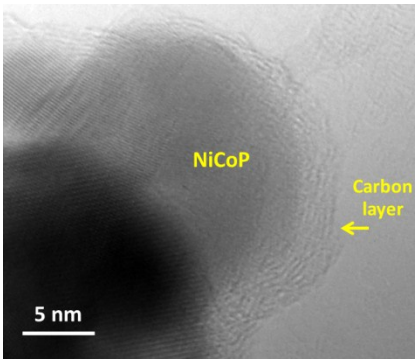

Figure S12. TEM image of NiCoP-C(TPA)/NF.

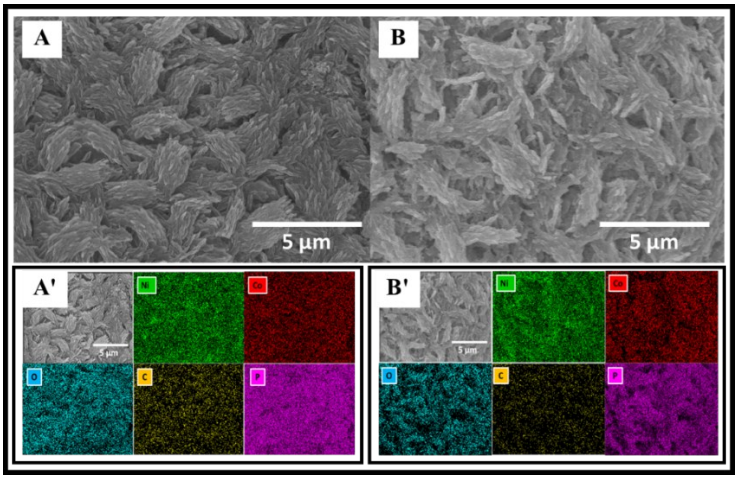

Figure S13. SEM image of NiCoP-C(TPA)/NF (A) fresh catalyst (B) after stability test 20h EDS mapping of NiCoP-C(TPA)/NF (A') before test and (B') after test stability test in 1M KOH electrolyte.

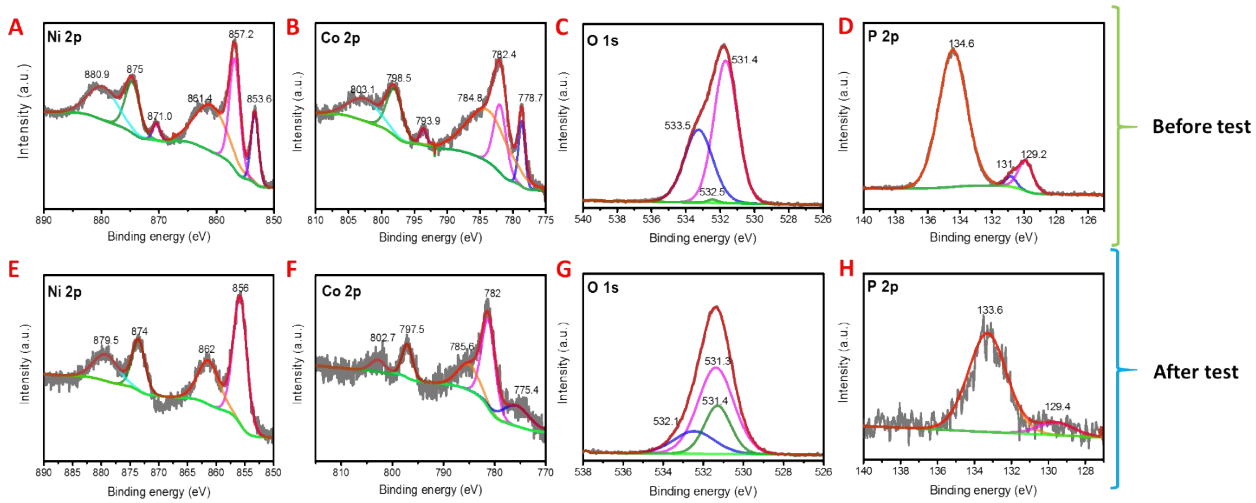

Figure S14. High-resolution XPS spectra of NiCoP-C(TPA) of (A-D) before HER test and (E-H) after HER test in the alkaline media solution.

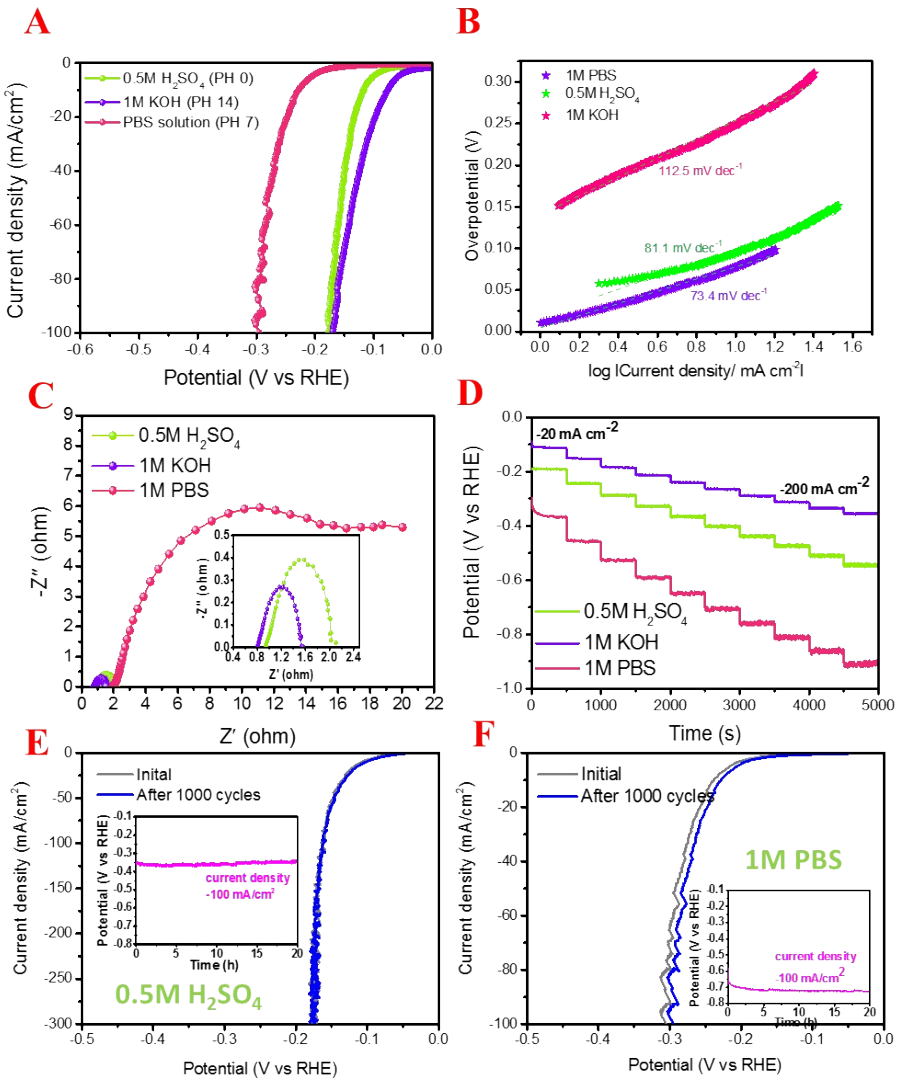

Figure S15. HER performances of NiCoP-C(TPA)/NF in acidic, neutral and alkaline electrolytes. (A) LSV curves. (B) Tafel plots. (C) Nyquist plots at an overpotential of 200 mV and (D) Multi-current step started at a current density of -20 mA cm^{-2} and ended at -200 mA cm^{-2} with an increment of 20 mA cm^{-2} every 500 sec. (E, F) Chronopotentiometry of NiCoP-C(TPA)/NF at a current density of -100 mA cm^{-2} duration a period of 20 h in (E) 0.5 M H_2SO_4 (pH=0). (F) 1M PBS (pH=7).

References

1. W. Ahn, M. G. Park, D. U. Lee, M. H. Seo, G. Jiang, Z. P. Cano, F. M. Hassan, Z. Chen, Adv. Funct. Mater., 2018, 28, 1802129.

2. X. Liang, B. Zheng, L. Chen, J. Zhang, Z. Zhuang, B. Chen, ACS Appl. Mater. Interfaces, 2017, 9, 23222-23229.

3. J. Yu, Q. Li, N. Chen, C.-Y. Xu, L. Zhen, J. Wu, V. P. Dravid, ACS Appl. Mater. Interfaces, 2016, 8, 27850-27858.

4. Y. Feng, X.-Y. Yu, U. Paik, ChemComm., 2016, 52, 1633-1636.

5. C. Du, L. Yang, F. Yang, G. Cheng, W. Luo, ACS Catalysis, 2017, 7, 4131-4137.

6. P. Jiang, Q. Liu, X. Sun, Nanoscale, 2014, 6, 13440-13445.

7. D. Liu, Q. Lu, Y. Luo, X. Sun, A. M. Asiri, Nanoscale 2015, 7, 15122-15126.

8. C. Tang, L. Gan, R. Zhang, W. Lu, X. Jiang, A. M. Asiri, X. Sun, J. Wang, L. Chen, Nano Letters, 2016, 16, 6617-6621.

9. J. Song, C. Zhu, B. Z. Xu, S. Fu, M. H. Engelhard, R. Ye, D. Du, S. P. Beckman, Y. Lin, Adv. Energy Mater., 2017, 7, 1601555.

10. X. Li, S. Li, A. Yoshida, S. Sirisomboonchai, K. Tang, Z. Zuo, X. Hao, A. Abudula, G. Guan, Catal. Sci. Technol., 2018, 8, 4407-4412.

11. Y. Li, J. Liu, C. Chen, X. Zhang, J. Chen, ACS Appl. Mater. Interfaces, 2017, 9, 5982-5991.

12. J. Wei, M. Zhou, A. Long, et al., Nano-Micro Lett, 2018, 10 (75), 2311-6706.

13. T. Shinagawa, A. T. Garcia-Esparza, K. Takanabe, Sci Rep. 2015, 5, 13801.

14. Y. Liu, H. Yu, X. Quan, S. Chen, H. Zhao, Y. Zhang, Sci Rep. 2014, 4, 6843.